JMEPEG (2017) 26:4282–4290
DOI: 10.1007/s11665-017-2897-y

1059-9495/$19.00

Preparation of Phytic Acid/Silane Hybrid Coating on Magnesium Alloy and Its Corrosion Resistance in Simulated Body Fluid

Fengwu Wang, Shu Cai, Sibo Shen, Nian Yu, Feiyang Zhang, Rui Ling, Yue Li, and Guohua Xu

(Submitted November 25, 2016; in revised form April 21, 2017; published online September 5, 2017)

In order to decrease the corrosion rate and improve the bioactivity of magnesium alloy, phytic acid/saline hybrid coatings were synthesized on AZ31 magnesium alloys by sol–gel dip-coating method. It was found that the mole ratio of phytic acid to γ-APS had a great influence on coating morphology and the corresponding corrosion resistance of the coated magnesium alloys. When the mole ratio of phytic acid to γ-APS was 1:1, the obtained hybrid coating was integral and without cracks, which was ascribed to the strong chelate capability of phytic acid and Si-O-Si network derived from silane. Electrochemical test result indicated that the corrosion resistance of the coated magnesium alloy was about 27 times larger than that of the naked counterpart. In parallel, immersion test showed that the phytic acid/silane hybrid coating could induce CaP-mineralized product deposition, which offered another protection for magnesium alloy.

Keywords corrosion resistance, hybrid coating, magnesium alloy, phytic acid, silane

1. Introduction

Biomedical implants used to repair or replace injured bone tissues should possess some properties, such as controlled degradation and favorable biochemical reactions (Ref 1, 2). Traditional implant materials, such as titanium and its alloys, have some drawbacks, such as poor bioactivity and mechanical property mismatching with the natural bones, which lead to long-term complications and need secondary surgery (Ref 3). The ideal implant materials should be bioactive to induce new bone formation, similar to natural bone mechanics, and have controlled degradation performance (Ref 4). In recent years, magnesium and magnesium alloys as promising degradable implants have gained increasing concern by virtue of many advantages: Magnesium is one of the most important elements for human metabolism, which could be absorbed after the implant degradation; their mechanical properties are similar to that of the compact bones, which could reduce the stress-shielding effect (Ref 5). However, the corrosion of magnesium in the physiological environment is very fast, resulting in the deterioration of mechanical property, especially for load-bearing implants (Ref 6). In addition, due to the rapid corrosion, local environment alkalization and rapid hydrogen releasing would bring about adverse effect to tissue healing. In general, the methods applied to improve the corrosion resistance of magnesium and magnesium alloys mainly can be divided into two categories: magnesium alloy processing (e.g., alloying or plastic deformation) and surface modification (e.g., preparation of protective coatings) (Ref 7-16). Among the two categories, surface modification is preferred. Through preparing protective coatings on magnesium and magnesium alloys, the substrates would be separated from the corrosive medium; thus, the corrosion rate could be controlled (Ref 16-18). Generally protective coatings on magnesium and magnesium alloys can be divided into conversion coatings and deposited coatings (Ref 19). Compared with deposited coatings, conversion coatings are in situ grown coatings which are formed by specific reactions between the substrates and environment. So conversion coatings seldom peel off from the substrates (Ref 20). However, most conversion coatings contain cracks, which are detrimental to the protective effect. One of the widely used conversion coatings (chromate conversion coating) could improve the corrosion resistance of magnesium and magnesium alloys, but hexavalent chromium ion has side effects to human body and environment (Ref 21, 22); thus, seeking a new kind of environmentally friendly and non-toxic conversion coating is highly desired.

Phytic acid is a kind of natural macromolecule, which is non-toxic and exists in most plant seeds. The hydrolysis products of phytic acid are inositol and phosphate, which are also harmless to environment and human body (Ref 13). Phytic acid contains 24 oxygen atoms, 12 hydroxyl and 6 phosphate groups, exhibiting a strong chelation with a variety of metal ions, so as to form phytic acid conversion coating on metallic implant surface for corrosion protection (Ref 13, 22-24). In recent years, phytic acid conversion coatings have caused wide concern. Cui et al. (Ref 25-27) found that magnesium alloy and phytic acid with a certain concentration could react and generate a magnesium phytic acid layer, which improved the corrosion resistance and biological property of magnesium

Fengwu Wang, Shu Cai, Nian Yu, Feiyang Zhang, Rui Ling, and **Yue Li**, Key Laboratory for Advanced Ceramics and Machining Technology of Ministry of Education, Tianjin University, Tianjin 300072, People's Republic of China; **Sibo Shen**, Center for Electron Microscopy, Institute for New Energy Materials and Low-Carbon Technologies, Tianjin University of Technology, Tianjin 300384, People's Republic of China; and **Guohua Xu**, Shanghai Changzheng Hospital, Shanghai 200003, People's Republic of China. Contact e-mails: caishu@tju.edu.cn, xuguohuamail@163.com, and wfwtju@163.com.

alloy. However, phytic acid conversion coatings also have some drawbacks. The coatings are very thin and easy to crack due to the use of aqueous precursors; thus, the protective effect is not satisfactory during the process of in vitro immersion test (Ref 22, 28, 29).

Silane coupling agent is a kind of organic silicon compound with special structure. The general formula of silanes could be expressed as $X_3Si(CH_2)_nY$ (Ref 30). In the formula, Y is organofunctional groups, such as vinyl, amino, glycidyl and hydroxyl, which could react with polymers; X stands for a hydrolysable alkoxy group. It is generally accepted that the hydrolysis of alkoxy groups in silane solution generates silanol groups (Si-OH), which could react with hydroxides and form strong Si-O-Me bonds, when these silanol groups contact with hydroxyl-covered metal surface. The interfacial Si-O-Me bonds and condensed Si-O-Si bonds in silane coating matrix construct a highly cross-linked three-dimensional network, which endows silane as an effective protection coating for metallic implants (Ref 30-33).

Generally speaking, single polymer coating is unsatisfactory for the corrosion protection of magnesium and magnesium alloys. In order to improve the corrosion resistance and bioactivity, a kind of hybrid coating structure consisting of silane and phytic acid was designed on magnesium alloy. Silanol could improve the integrity of the hybrid coating via forming Si-O-Me, Si-O-Si and Si-O-P bonds (Ref 23, 30-33). In parallel, phytic acid could enhance the bioactivity (Ref 13).

2. Materials and Methods

2.1 Substrate Pretreatment

Magnesium alloys used in this work were cut from commercial AZ31 magnesium alloy plates (Al 3%, Zn 1%, Mn 0.2%, Fe $<$ 0.005% and balanced Mg, all in wt.%). First, the substrates with approximate size of 10 mm $\times$ 10 mm $\times$ 2 mm were polished with SiC papers to 2000 grit. Then, the substrates were ultrasonically cleaned in distilled water, ethanol and acetone for 15 min, respectively. Next, the substrates were immersed in 3 M NaOH solution at 80 °C for 1 h. Finally, the substrates were rinsed with deionized water and dried in hot air.

2.2 Coating Preparation

First, phytic acid and γ-APS (mole ratios were 1:1, 1:2 and 2:1, respectively) were added into 40 ml mixed solution with water/ethanol volume ratio of 3:2 under continuous magnetic stirring at 20 °C for 30 min to obtain homogeneous sols; meanwhile, the pH value of the sols was adjusted to 8.0 using NaOH solution. Then, the sols were heated up to 35 °C for 1.5 h. Next, alkaline-treated substrates were immersed into different sols and aged for 24 h, dried at 30 °C for 24 h and heat-treated at 100 °C for 1 h.

2.3 Coating Characterization

The surface morphology before and after immersion in simulated body fluid (SBF) and the chemical composition of phytic acid/silane hybrid coatings were characterized using field emission scanning electron microscope (FE-SEM, JOEL 6700F, Japan) equipped with energy dispersive spectroscopy (EDS, 7401 Oxford). The chemical structure of phytic acid/silane hybrid coatings were measured using Fourier transform infrared spectroscopy (FTIR, Nicolet 6700, USA) in the spectral range 400-4000 cm^{-1}.

2.4 Electrochemical Test

A classical three-electrode cell with platinum electrode as counter electrode, saturated calomel electrode as reference electrode and the naked and coated magnesium alloys with an exposed area of 100 mm^2 as working electrode were used to evaluate the corrosion protection of phytic acid/silane hybrid coatings for magnesium alloys. Electrochemical impedance spectroscopy (EIS) and potentiodynamic polarization were measured in SBF at 37 °C (CHI600C, China). Ion concentrations of the SBF are 5.0 mM K^+, 142.0 mM Na^+, 2.5 mM Ca^{2+}, 1.5 mM Mg^{2+}, 4.2 mM HCO_3^{2-}, 147.8 mM Cl^-, 0.5 mM SO_4^{2-} and 1.0 mM HPO_4^{2-}. Tris–HCl was used as a buffer solution to maintain a constant pH value of 7.40. Before conducting the electrochemical test, the samples were immersed into SBF for 10 min to attain a stable open-circuit potential. The EIS test was performed at scan frequency ranging from 100 kHz to 0.01 Hz with the amplitude of 10 mV. The polarization test was conducted at scan rate of 1.0 mV/s. Three parallel samples were measured to ensure repeatability.

2.5 In Vitro Immersion Test

To investigate the long-term corrosion protection and bioactivity of phytic acid/silane hybrid coatings, in vitro immersion test was carried out in SBF at 37 °C (pH 7.40). The SBF was refreshed every 2 days during the immersion period up to 9 days. The volume of SBF was calculated as volume to sample area of 20 mL/cm^2, according to ASTM G31-72 (Ref 34). After immersion test, the samples were removed from the SBF, washed gently with distilled water and dried in air at room temperature. Simultaneously, pH value of the SBF was determined by a pH meter (PB-10, China). To measure the mass loss of magnesium alloy, the corrosion products and mineralization products on the coated and naked magnesium alloys were removed by chromic acid solution ($K_2Cr_2O_7$ and H_2SO_4). The mass loss was calculated as follows:

$$\text{Mass loss} = (m_0 - m_1)/S \quad \text{(Eq 1)}$$

where m_0 is the mass of sample before immersion, m_1 is the mass of sample after immersion, S is the surface area of magnesium alloy. Three parallel measurements were conducted for each sample, and the average and deviation were calculated.

3. Results and Discussion

3.1 Surface Morphology and Chemical Composition of Phytic Acid/Silane Hybrid Coatings

The integrity of protective coatings is key factor influencing the corrosion protection performance. As illustrated in Fig. 1(a) and (b), when the mole ratio of phytic acid to γ-APS was 1:1, integral and crack-free phytic acid/silane hybrid coating was prepared on magnesium alloy. When the mole ratio of phytic acid to γ-APS was 1:2, the hybrid coating surface displayed white deposits and pores under low-magnification image

(Fig. 1d and e). When the mole ratio of phytic acid to γ-APS was 2:1, the hybrid coating cracked (Fig. 1g and h). It was noting that the morphology of the hybrid coatings with mole ratios of phytic acid to γ-APS of 1:1 and 1:2 showed no obvious difference under high-magnification images (Fig. 1b and e). But when the mole ratio of phytic acid to γ-APS was 2:1, the hybrid coating surface showed some micro-cracks, which might be formed by the dehydration in the SEM vacuum chamber (Fig. 1h). As shown in the EDS spectrum in Fig. 1(c), the P/Si mole ratio was around 6, which was due to that a phytic acid molecule contains 6 phosphate groups, and silane is a single organoalkoxysilane, indicating the full reaction of phytic acid and silane. However, the P/Si mole ratios were different when the mole ratios of phytic acid to γ-APS were 1:2 and 2:1. A few deposits and cracks presented on the hybrid coating surface (Fig. 1d and g), meaning incomplete reaction between phytic acid and silane; thus, the P/Si mole ratios were below 6 (Fig. 1f and i). Furthermore, all EDS spectra in Fig. 1 exhibited relatively high intensity of magnesium peak compared with that of P and Si, which might be attributed to the low thickness of the hybrid coatings.

3.2 Electrochemical Property of the Coated and Naked Magnesium Alloys

To evaluate the protective effect of phytic acid/silane hybrid coatings, electrochemical test including potentiodynamic polarization and electrochemical impedance was carried out. Figure 2 shows the potentiodynamic polarization curves of the coated and naked magnesium alloys. Corrosion potential (E_{corr}) and corrosion current density (i_{corr}) extracted from the curves using Tafel extrapolation method (Ref 9) are listed in Table 1. Compared with the naked magnesium alloy, the increase in E_{corr} and decrease in i_{corr} of the coated magnesium alloys demonstrated that phytic acid/silane hybrid coatings could provide effective protection for magnesium alloys in SBF. It could be seen that, with the mole ratio of phytic acid to γ-APS changing, E_{corr} did not changed obviously; however, i_{corr} changed significantly. i_{corr} of the coated magnesium alloys with mole ratio of phytic acid to γ-APS of 1:1 was 3.57 μA/cm^2, smaller than that with mole ratio of phytic acid to γ-APS of 1:2 (4.44 μA/cm^2) and 2:1 (3.95 μA/cm^2), indicating that the coated magnesium alloy with mole ratio of phytic acid to γ-APS of 1:1 showed the best corrosion resistance. E_{corr} of the coated magnesium alloy with mole ratio of phytic acid to γ-APS of 1:1 was −1.61 V, larger than that of the naked magnesium alloy (−1.70 V).

In general, the diameter of capacitive loop in Nyquist plots represents the polarization resistance of the working electrode (Ref 35, 36). In this work, the polarization resistance of the naked and coated magnesium alloys with mole ratios of phytic acid to γ-APS of 1:1, 1:2 and 2:1 was 507, 13,835, 9205 and 9650 Ω cm^2, respectively (Fig. 3). The increase in impedance indicated that the coated magnesium alloys showed better corrosion resistance compared with the naked counterpart. The coated magnesium alloy with mole ratio of phytic acid to γ-APS of 1:1 showed the best corrosion resistance, and the corresponding impedance was about 27 times larger than that of

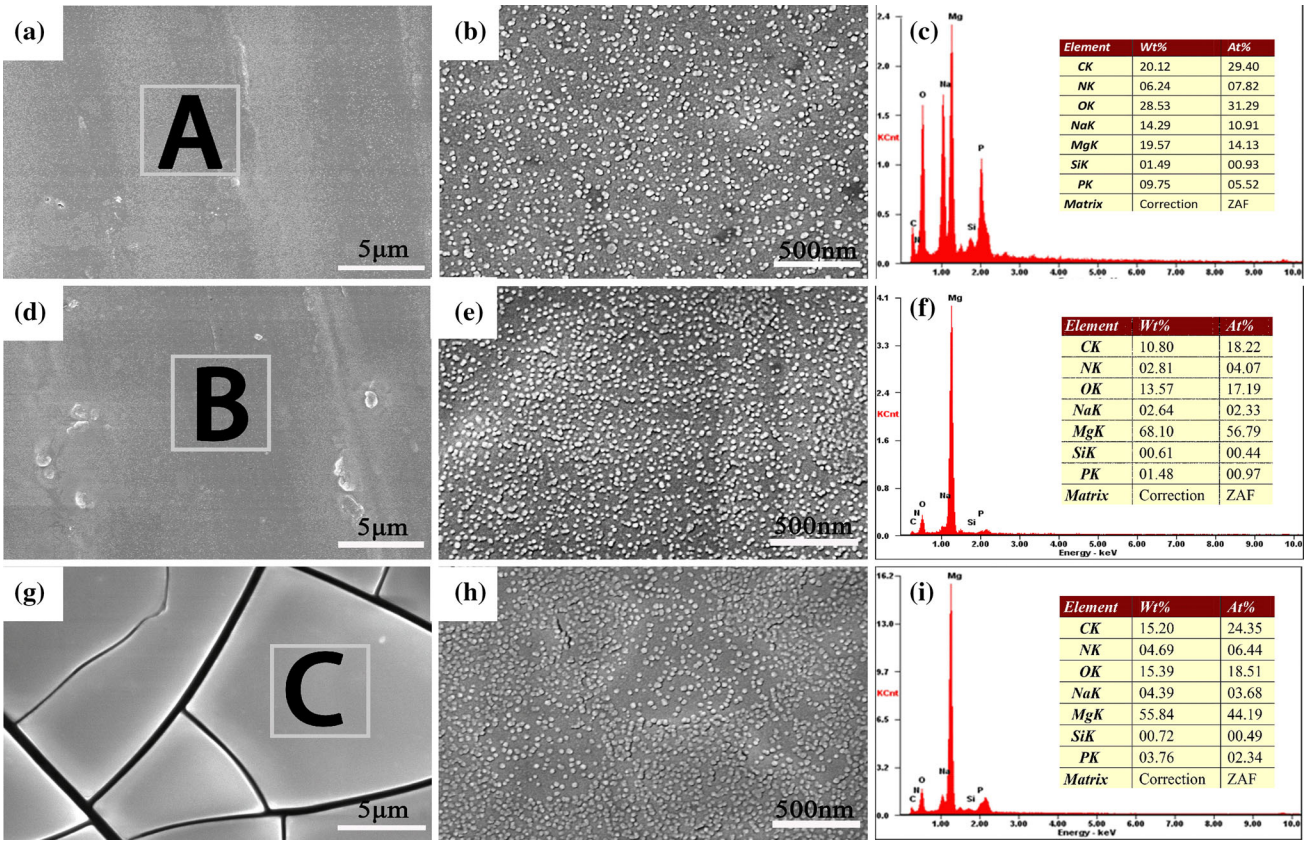

Fig. 1 FE-SEM images of the surface morphologies of phytic acid/silane hybrid coatings with different mole ratios: (a–b) mole ratio of 1:1, (d–e) mole ratio of 1:2, (g–h) mole ratio of 2:1. (c) EDS spectrum of area A in (a), (f) EDS spectrum of area B in (d) and (i) EDS spectrum of area C in (g)

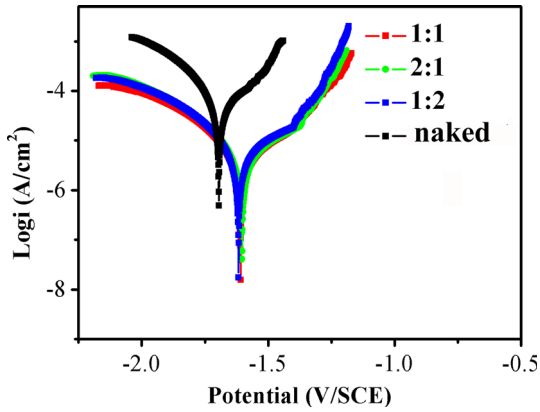

Fig. 2 Potentiodynamic polarization curves of the coated and naked magnesium alloys

Table 1 Corrosion potentials and corrosion current densities of the coated and naked magnesium alloys

Samples	E_{corr} (V/SCE)	i_{corr} (μA/cm^2)
1:1	−1.61	3.57
1:2	−1.62	4.44
2:1	−1.60	3.95
Naked	−1.70	49.41

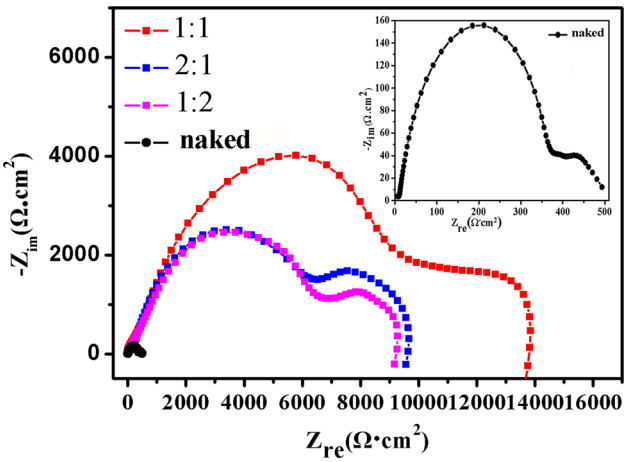

Fig. 3 Nyquist plots of the naked and coated magnesium alloys with different mole ratios of phytic acid to γ-APS. The inset showed the Nyquist plot of the naked magnesium alloy

the naked magnesium alloy. The result was consistent with the potentiodynamic polarization results (Fig. 2; Table 1). The Nyquist plots of all samples could be divided into two well-defined loops at both high- and medium-frequency regions. The high-frequency capacitive loop was related to the charge transfer reaction in the electric double layer, and the medium-frequency capacitive loop was attributed to the mass transfer in corrosion product layer (Ref 4, 22, 35, 36).

The coated magnesium alloy with mole ratio of phytic acid to γ-APS of 1:1 exhibited the best corrosion resistance among the three samples, which was attributed to the integral coating

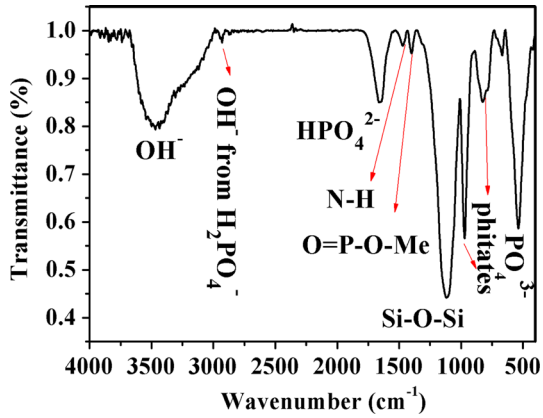

Fig. 4 FTIR spectrum of phytic acid/silane hybrid coating with mole ratio of 1:1

structure, so as to effectively retard the permeation of SBF into the coating to contact magnesium alloy. It was expected that the hybrid coating was able to reduce the corrosion rate of magnesium alloy, which was important for maintaining the mechanical strength of magnesium alloy implant in the initial healing process.

3.3 Chemical Structure of Phytic Acid/Silane Hybrid Coating

The hybrid coating with phytic acid to γ-APS of 1:1 was integral and the corrosion resistance was the largest among the three samples, so it was selected to conduct FTIR measurement to detect the coating structure and chemical groups. There were four characteristic vibration bands: hydroxyl (OH^-) at 3400 and 3000 cm^{-1}, phosphate radical (PO_4^{3-}) at 539 cm^{-1}, phosphate hydrogen radical (HPO_4^{2-}) at 1656 cm^{-1} and phytate bands at 1500 and 950 cm^{-1} (Fig. 4). All the bands were corresponding to the chelate compounds between magnesium alloy and phytic acid (Ref 23, 27, 29, 36). The above result was in line with our previous and others' works (Ref 24, 37). In addition, two new bands existed at 1520 and 1200 cm^{-1}, which were assigned to N-H and Si-O-Si groups (Ref 30, 38), suggesting that silane formed a network structure during the coating preparation. The presence of N-H was in accordance with other reports, in which a new band around 1570 cm^{-1} was assigned to protonated amino groups (Ref 30, 39). Our previous work (Ref 23) indicated that Si-OH produced by silane hydrolysis could react with P-OH in phytic acid. However, in the present work, the relatively weak Si-O-P band might be covered by the strong Si-O-Si band.

3.4 In Vitro Degradation and Mineralization of the Coated Magnesium Alloy

The coated magnesium alloy with mole ratio of phytic acid to γ-APS of 1:1 exhibited the best corrosion resistance, so it was selected to conduct in vitro immersion test. Figure 5 reveals the surface morphology and chemical composition of the hybrid coating after immersion for different days. After immersion for 2 days, the hybrid coating was partly dissolved and cracks were formed on the coating surface (Fig. 5a). Meanwhile, the dissolved area provided nucleation sites for mineralized precipitates. In the enlarged view, some spherical mineralized precipitates deposited in the cracked area (Fig. 5b) and the Ca/P mole ratio was 0.84 (Fig. 5c). After immersion for 6 days, the hybrid coating was further dissolved and the cracks

on the coating surface became obvious and the crack width increased (Fig. 5d). In the enlarged view, spherical mineralized precipitates grew larger and aggregated (Fig. 5e). Meanwhile, the Ca/P mole ratio increased to 0.94 (Fig. 5f). After immersion for 9 days, there was no further increasing for the crack width (Fig. 5g). In the enlarged view, some plate-like mineralized precipitates were formed (Fig. 5h) and the Ca/P mole ratio was further increased to 0.96 (Fig. 5i). The plate-like precipitates and spherical precipitates together constructed CaP-mineralized layer, which was expected to provide another protection for magnesium alloy.

In vitro immersion test provided long-term corrosion protection information of the hybrid coatings. The mass loss of the coated and naked magnesium alloys as well as the pH variation of the SBF was examined, and the results are illustrated in Fig. 6 and 7, respectively. After immersion for 2 days, the mass loss of the naked and coated magnesium alloys was 8.13 and 4.85 mg/cm^2, respectively. In parallel, the SBF with the coated magnesium alloy showed a lower pH value of 7.78 compared with that with the naked counterpart of 8.52. After immersion for 6 days, the mass loss of the coated magnesium alloy showed a slight increase to 7.74 mg/cm^2, while the naked counterpart displayed a sharp increase to 52.32 mg/cm^2. The pH value of the SBF with the naked magnesium alloy reached to 9.80, while the pH value of the SBF with the coated magnesium alloy maintained almost stable and reached to 7.86. After immersion for 9 days, the mass loss of the naked magnesium alloy rose to 95.35 mg/cm^2, while the coated magnesium alloy showed lower mass loss of 11.96 mg/cm^2 and the pH value was about 8.02, indicating that the hybrid coating could effectively improve the corrosion resistance of magnesium alloy in SBF.

To quantify the corrosion resistance of the coated magnesium alloy after immersion in SBF for different periods, potentiodynamic polarization test was performed on the immersed samples and the results are shown in Fig. 8 and Table 2. E_{corr} of the coated magnesium alloy after immersion for different periods was higher than that of the naked magnesium alloy (−1.70 V). Analogously, i_{corr} of the coated magnesium alloy after immersion for different periods was lower than that of the naked magnesium alloy (49.41 μA/cm^2).

For further understanding the corrosion resistance of the coated magnesium alloy during immersion test, EIS analysis was conducted. The fitting circuit for the Nyquist plots of the coated magnesium alloy after immersion for different periods is illustrated in Fig. 9. The equivalent circuit was comprised of resistance of electrolyte (R_s), charge transfer resistance (R_t), corrosion product layer resistance (R_{corr}) and corrosion product layer capacitance (CPE). After immersion from 2 to 9 days, as shown in Table 3, R_t of the coated magnesium alloy changed from

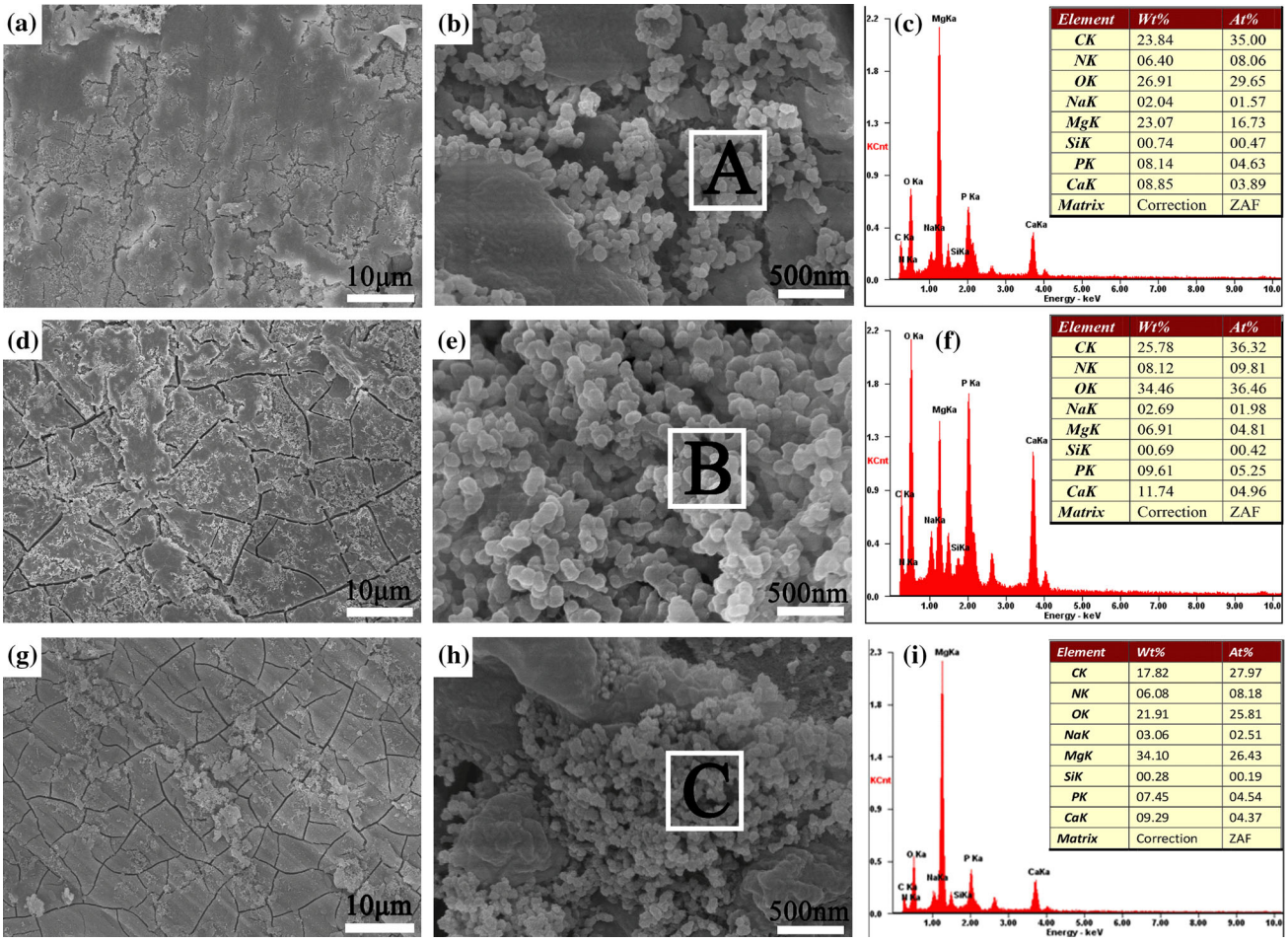

Fig. 5 FE-SEM images of the surface morphologies of phytic acid/silane hybrid coatings after immersion in SBF for different periods: (a–b) 2 days, (d–e) 6 days and (g–h) 9 days. (c) EDS spectrum of area A in (b), (f) EDS spectrum of area B in (e) and (i) EDS spectrum of area C in (h)

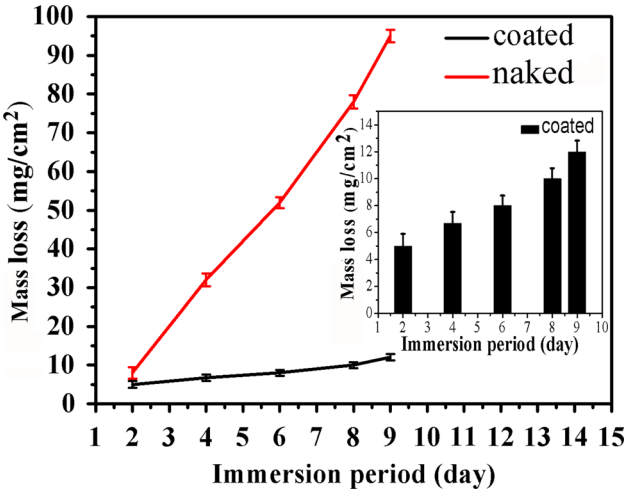

Fig. 6 Mass loss of the coated and naked magnesium alloys after immersion in SBF for different periods

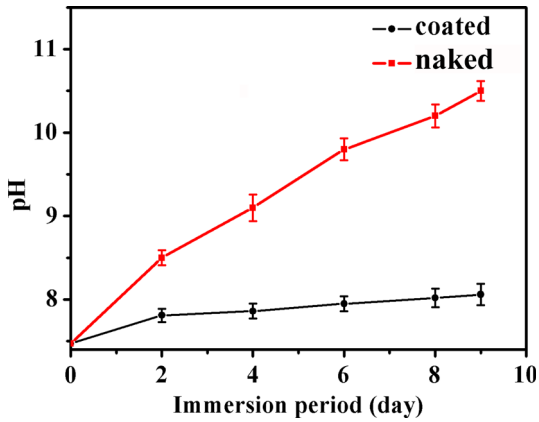

Fig. 7 pH variation of the SBF after immersion for different periods

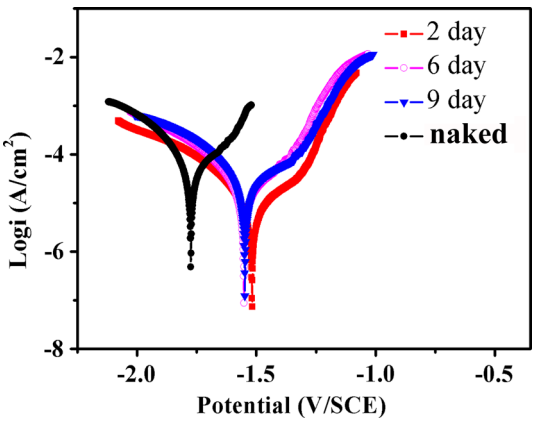

Fig. 8 Potentiodynamic polarization curves of the coated and naked magnesium alloys after immersion for different periods

1426.04 to 575.24 Ω cm^2 and finally declined to 493.23 Ω cm^2, which were higher than that of the naked magnesium alloy (119.36 Ω cm^2), proving the effective protection of the hybrid coating to magnesium alloy. The gradual decrease in R_t was due to coating dissolution. Meanwhile, R_{corr} of the coated magnesium

Table 2 Corrosion potentials and corrosion current densities of the coated and naked magnesium alloys after immersion in SBF for different periods

Samples	E_{corr} (V/SCE)	i_{corr} (μA/cm^2)
2 days	−1.52	7.60
6 days	−1.55	20.73
9 days	−1.55	16.74
Naked	−1.70	49.41

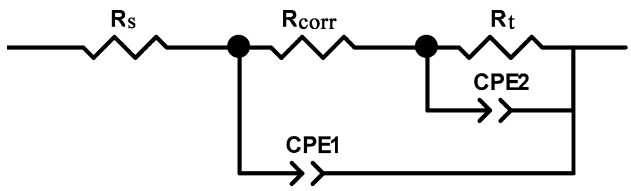

Fig. 9 Equivalent circuit for the Nyquist plots

alloy first decreased and then increased, which was due to the formation of CaP-mineralized precipitates.

Therefore, the mass loss of the coated and naked magnesium alloys, pH variation of the SBF, potentiodynamic polarization and EIS test results together demonstrated that phytic acid/silane hybrid coating and the formed CaP-mineralized precipitates after immersion in SBF could offer effective protection for magnesium alloy.

Phytic acid has strong chelate capability, which could form stable chelate compounds and chemical bonding with magnesium alloy (Ref 23, 36, 40). In addition, silane generated Si-OH through hydrolysis, which could chemically bond with magnesium alloy, in parallel, could condense to form Si-O-Si 3D network (Ref 30). Generally speaking, the existence of the above structures could result in integral hybrid coating. However, the volume of both phytic acid and silane were relatively large and the space steric effect was significant. So in the coating preparation, the different mole ratios of the two reactants would produce different coating structure containing magnesium phytic acid and Si-O-Si 3D network. When phytic acid content in the precursor sol was excessive, magnesium phytic acid was more than the Si-O-Si network in the hybrid coating. So the hybrid coating structure was similar to pure magnesium phytic acid coating, and the surface of the hybrid coating had a large number of cracks (Fig. 1g). While silane was overdosed, the corresponding content of Si-O-Si network was larger than that of magnesium phytic acid, which could produce many white particles on the hybrid coating (Fig. 1b). Only the precursor sol with appropriate mole ratio of phytic acid to γ-APS was used; smooth, integral and crack-free hybrid coating was obtained (Fig. 1a).

Protective coating as a physical barrier separating magnesium alloy from corrosion solution improved the corrosion resistance (Ref 41). Integral and crack-free protective coating would enhance this protective effect. Based on the electrochemical test result, the hybrid coating with mole ratio of phytic acid to γ-APS of 1:1 had the best corrosion resistance (maximum impedance and minimum i_{corr}), and this hybrid coating was chosen to execute the in vitro immersion test. After immersion for 2 days, the hybrid coating was partly dissolved and cracked, which might be caused from the hydrolyzation of

Table 3 Data of fitting results of equivalent circuit for the Nyquist plots

Samples	R_s, Ω cm^2	R_{corr}, Ω cm^2	R_t, Ω cm^2	CPE2-T, S s^n/cm^2	CPE2-P, S s^n/cm^2	CPE1-T, S s^n/cm^2	CPE1-P, S s^n/cm^2
2 days	32.78	3000.03	1426.04	3.21E−4	0.77	4.39E−6	0.82
6 days	36.65	984.35	575.24	5.02E−4	0.79	5.98E−6	0.85
9 days	30.63	1290.31	493.23	3.48E−4	0.91	4.99E−6	0.78
Naked	12.23	363.92	119.36	4.45E−2	0.68	1.04E−5	0.89

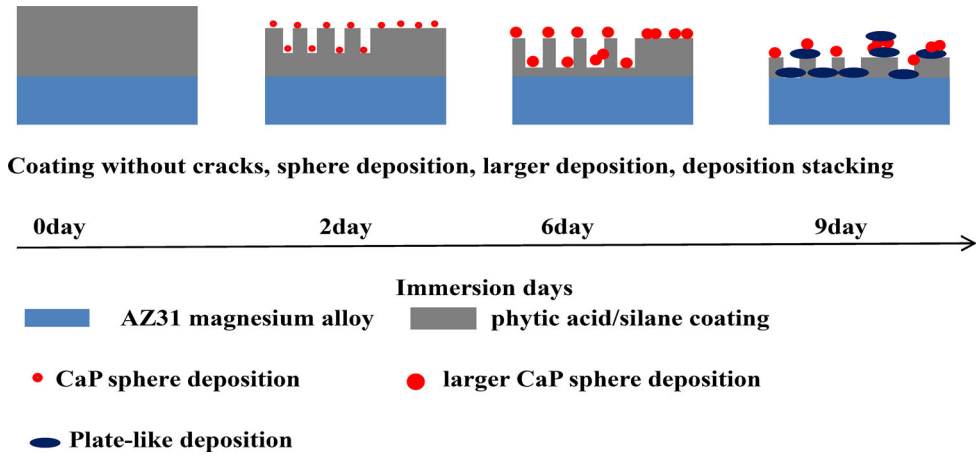

Fig. 10 Schematic illustration of the corrosion process of phytic acid/silane hybrid coating on magnesium alloy in SBF

Si-O-Si and Si-O-P bonds in the hybrid coating (Ref 42). Moreover, the coating cracks might be caused from the tensile stress and thermal stress produced during the heat treatment (Ref 43, 44). Magnesium phytic acid as a relatively stable chelate compound was beneficial for human physiology and would be taken into the physiological environment through partly hydrolysis of the hybrid coating. It was found from the macroscopic image that, the hybrid coatings did not peel off, which might be caused by the strong bonding between the coating and substrate (Ref 45). Even though the hybrid coating was partly dissolved and cracked, phosphorus hydroxyl produced by hydrolysis provided active sites for calcium phosphate-mineralized precipitates deposition (Ref 46). For SBF was supersaturated with respect to apatite (Ref 47), some spherical mineralized precipitates deposited in the region of the dissolved area, meaning that the hybrid coating had good bioactivity (Ref 47). The hybrid coating contained much phosphorus hydroxyl and magnesium phytic acid, so the Ca/P ratio was lower than the stoichiometric ratio of hydroxyapatite. After dissolution of the hybrid coating, the SBF was abounded with phosphate groups. After 6-day immersion, spherical CaP-mineralized precipitates grew up and became a loose accumulation. After immersion for 9 days, plate-like CaP-mineralized precipitates accumulated on the former sphere CaP precipitates and the Ca/P ratio of 1 was lower than 1.67, which was due to that magnesium ion inhibited the crystallization of CaP (Ref 48-51). The increase of phosphate groups in SBF also played a role in forming calcium-deficient phosphate compounds. During the process of immersion test, the mass loss of the coated magnesium alloy kept slowly rising. After 9-day immersion, the mass loss of the coated magnesium alloy was the same with that of the naked magnesium alloy after 1-day immersion.

To sum up, the corrosion process of phytic acid/silane hybrid coating on magnesium alloy in SBF is depicted in Fig. 10. First, the initial integral hybrid coating was dissolved and some cracks were formed on the coating surface; meanwhile, sphere CaP-mineralized precipitates were formed on the dissolved area. Then, the sphere CaP-mineralized precipitates grew larger and the coating continued dissolving, but without peeling off. Finally, the hybrid coating was dissolved deeply to the magnesium alloy; thus, corrosion occurred and plate-like CaP-mineralized precipitates were formed and stacked on the larger sphere CaP-mineralized precipitates, which offered another protection for the magnesium alloy.

4. Conclusion

In this work, phytic acid/silane hybrid coatings were prepared on magnesium alloys through sol–gel dip-coating method to improve the corrosion resistance and bioactivity. The mole ratio of silane to phytic acid played a significant role on the coating morphology and corrosion resistance of samples. When the mole ratio of phytic acid to γ-APS was 1:1, the hybrid coating was integral and crack-free. The corrosion resistance of the coated magnesium alloy improved approximately 27 times larger than that of the naked counterpart in SBF. Immersion test showed that, with the increasing of immersion time in SBF, due to the chemical bonds in the hybrid coating hydrolysis, the hybrid coating was progressively dissolved but without peeling off. Moreover, the dissolved area induced CaP-mineralized layer deposition and growth, which could provide further corrosion protection for magnesium alloy. The above results revealed that phytic acid/silane

hybrid coating is a promising protective coating on magnesium and magnesium alloys for orthopedic application.

Acknowledgments

The work was financially supported by the National Natural Science Foundation of China (Project Nos. 51372166, 51572186 and 81271954) and Tianjin Natural Science Foundation (Grant No. 15JCYBJC47500).

References

1. S. Hesaraki, M. Safari, and M.A. Shokrgozar, Composite Bone Substitute Materials Based on Beta-Tricalcium Phosphate and Magnesium-Containing Sol-Gel Derived Bioactive Glass, *J. Mater. Sci. Mater. Med.*, 2009, **20**, p 2011–2017
2. T.T. Roberts and A.J. Rosenbaum, Bone Grafts, Bone Substitutes and Orthobiologics the Bridge Between Basic Science and Clinical Advancements in Fracture Healing, *Organogenesis*, 2012, **8**, p 114–124
3. Y. Dou, S. Cai, X.Y. Ye, G.H. Xu, H.T. Hu, and X.J. Ye, Preparation of Mesoporous Hydroxyapatite Films Used as Biomaterials Via Sol-Gel Technology, *J. Solgel Sci. Technol.*, 2012, **61**, p 126–132
4. S.B. Shen, S. Cai, G.H. Xu, H. Zhao, S.X. Niu, and R.Y. Zhang, Influence of Heat Treatment on Bond Strength and Corrosion Resistance of Sol-Gel Derived Bioglass-Ceramic Coatings on Magnesium Alloy, *J. Mech. Behav. Biomed.*, 2015, **45**, p 166–174
5. M.P. Sealy, Y.B. Guo, R.C. Caslaru, J. Sharkins, and D. Feldman, Fatigue Performance of Biodegradable Magnesium–Calcium Alloy Processed by Laser Shock Peening for Orthopedic Implants, *Int. J. Fatigue*, 2016, **82**, p 428–436
6. S.B. Shen, S. Cai, M. Zhang, G.H. Xu, Y. Li, R. Ling, and X.D. Wu, Microwave Assisted Deposition of Hydroxyapatite Coating on a Magnesium Alloy with Enhanced Corrosion Resistance, *Mater. Lett.*, 2015, **159**, p 146–149
7. A. Kurella and N.B. Dahotre, Review Paper: Surface Modification for Bioimplants: The Role of Laser Surface Engineering, *J. Biomater. Appl.*, 2005, **20**, p 5–50
8. M. Bakir, Haemocompatibility of Titanium and Its Alloys, *J. Biomater. Appl.*, 2012, **27**, p 3–15
9. M.G. Ren, S. Cai, T.L. Liu, K. Huang, X.X. Wang, H. Zhao, S.X. Niu, R.Y. Zhang, and X.D. Wu, Calcium Phosphate Glass/MgF_2 Double Layered Composite Coating for Improving the Corrosion Resistance of Magnesium Alloy, *J. Alloys Compd.*, 2014, **591**, p 34–40
10. L.L. Chen, Y.H. Gu, L. Liu, S.J. Liu, B.B. Hou, Q. Liu, and H.Y. Ding, Effect of Ultrasonic Cold Forging Technology as the Pretreatment on the Corrosion Resistance of MAO Ca/P coating on AZ31B Mg Alloy, *J. Alloys Compd.*, 2015, **635**, p 278–288
11. Y.Q. Chen, G.J. Wan, J. Wang, S. Zhao, Y.C. Zhao, and N. Huang, Covalent Immobilization of Phytic Acid on Mg by Alkaline Pretreatment: Corrosion and Degradation Behavior in Phosphate Buffered Saline, *Corros. Sci.*, 2013, **75**, p 280–286
12. C.J. Wang, B.L. Jiang, M. Liu, and Y.F. Ge, Corrosion Characterization of Micro-arc Oxidization Composite Electrophoretic Coating on AZ31B Magnesium Alloy, *J. Alloys Compd.*, 2015, **621**, p 53–61
13. Y.Q. Chen, S. Zhao, B. Liu, M.Y. Chen, J.L. Mao, H.R. He, Y.C. Zhao, N. Huang, and G.L. Wan, Corrosion-Controlling and Osteo-Compatible Mg Ion-Integrated Phytic Acid (Mg-PA) Coating on Magnesium Substrate for Biodegradable Implants Application, *ACS Appl. Mater. Iiter.*, 2014, **6**, p 19531–19543
14. Z. Grubac, I.S. Roncevic, M. Metikos-Hukovic, R. Babic, M. Petravic, and R. Peter, Surface Modification of Biodegradable Magnesium Alloys, *J. Electrochem. Soc.*, 2012, **159**, p 253
15. J.X. Yang, F.Z. Cui, and I.S. Lee, Surface Modifications of Magnesium Alloys for Biomedical Applications, *Ann. Biomed. Eng.*, 2011, **39**, p 1857–1871
16. M. Razavi, M. Fath, O. Savabi, S.M. Razavi, B.H. Beni, D. Vashaee, and L. Tayebi, Controlling the Degradation Rate of Bioactive Magnesium Implants by Electrophoretic Deposition of Akermanite Coating, *Ceram. Int.*, 2014, **40**, p 3865–3872
17. A. Abdal-hay, N.A.M. Barakat, and J.K. Lim, Hydroxyapatite-Doped Poly(Lactic Acid) Porous Film Coating for Enhanced Bioactivity and Corrosion Behavior of AZ31 Mg Alloy for Orthopedic Applications, *Ceram. Int.*, 2013, **39**, p 183–195
18. A. Dey, R.U. Rani, H.K. Thota, A.K. Sharma, P. Bandyopadhyay, and A.K. Mukhopadhyay, Microstructural, Corrosion and Nanomechanical Behaviour of Ceramic Coatings Developed on Magnesium AZ31 Alloy by Micro Arc Oxidation, *Ceram. Int.*, 2013, **39**, p 3313–3320
19. H. Hornberger, S. Virtanen, and A.R. Boccaccini, Biomedical Coatings on Magnesium Alloys—A Review, *Acta Biomater.*, 2012, **8**, p 2442–2455
20. L. Lei, J. Shi, X. Wang, D. Liu, and H.G. Xu, Microstructure and Electrochemical Behavior of Cerium Conversion Coating Modified with Silane Agent on Magnesium Substrates, *Appl. Surf. Sci.*, 2016, **376**, p 161–171
21. S.B. Brachetti-Sibaja, M.A. Domínguez-Crespo, S.E. Rodil, and A.M. Torres-Huerta, Optimal Conditions for the Deposition of Novel Anticorrosive Coatings by RF Magnetron Sputtering for Aluminum Alloy AA6082, *J. Alloys Compd.*, 2014, **615**, p 437–443
22. M. Zhang, S. Cai, S.B. Shen, G.H. Xu, Y. Li, R. Ling, and X.D. Wu, In-Situ Defect Repairing in Hydroxyapatite/Phytic Acid Hybrid Coatings on AZ31 Magnesium Alloy by Hydrothermal Treatment, *J. Alloys Compd.*, 2016, **658**, p 649–656
23. Y. Li, S. Cai, G.H. Xu, S.B. Shen, M. Zhang, T. Zhang, and X.H. Sun, Synthesis and Characterization of a Phytic Acid/Mesoporous 45S5 Bioglass Composite Coating on a Magnesium Alloy and Degradation Behavior, *RSC Adv.*, 2015, **5**, p 25708–25716
24. H.W. Shi, E.H. Han, F.C. Liu, and S. Kallip, Protection of 2024-T3 Aluminium Alloy by Corrosion Resistant Phytic Acid Conversion Coating, *Appl. Surf. Sci.*, 2013, **280**, p 325–331
25. X.F. Cui, L.L. Lin, E.B. Liu, G. Jin, and J. Jin, Performance Evolution of Phytic Acid Conversion Film in the Forming Process, *Adv. Mech. Eng.*, 2015, **5**, p 740303
26. X.F. Cui, Q.F. Li, Y. Li, F.H. Wang, G. Jin, and M.H. Ding, Microstructure and Corrosion Resistance of Phytic Acid Conversion Coatings for Magnesium Alloy, *Appl. Surf. Sci.*, 2008, **255**, p 2098–2103
27. X.F. Cui, Y. Li, Q.F. Li, G. Jin, M.H. Ding, and F.H. Wang, Influence of Phytic Acid Concentration on Performance of Phytic Acid Conversion Coatings on the AZ91D Magnesium Alloy, *Mater. Chem. Phys.*, 2008, **111**, p 503–507
28. J. Chen, Y.W. Song, D.Y. Shan, and E.H. Han, Modifications of the Hydrotalcite Film on AZ31 Mg Alloy by Phytic Acid: The Effects on Morphology, Composition and Corrosion Resistance, *Corros. Sci.*, 2013, **74**, p 130–138
29. R.Y. Zhang, S. Cai, G.H. Xu, H. Zhao, Y. Li, X.X. Wang, K. Huang, M.G. Ren, and X.D. Wu, Crack Self-Healing of Phytic Acid Conversion Coating on AZ31 Magnesium Alloy by Heat Treatment and the Corrosion Resistance, *Appl. Surf. Sci.*, 2014, **313**, p 896–904
30. X. Liu, Z.L. Yue, T. Romeo, J. Weber, T. Scheuermann, S. Moulton, and G. Wallace, Biofunctionalized Anti-Corrosive Silane Coatings for Magnesium Alloys, *Acta Biomater.*, 2013, **9**, p 8671–8677
31. B.N. Zand and M. Mahdavian, Corrosion and Adhesion Study of Polyurethane Coating on Silane Pretreated Aluminum, *Surf. Coat. Technol.*, 2009, **203**, p 1677–1681
32. Y.Y. Yue, Z.X. Liu, T.T. Wan, and P.C. Wang, Effect of Phosphate–Silane Pretreatment on the Corrosion Resistance and Adhesive-Bonded Performance of the AZ31 Magnesium Alloys, *Prog. Org. Coat.*, 2013, **76**, p 835–843
33. M.Y. Jiang, L.K. Wu, J.M. Hu, and J.Q. Zhang, Silane-Incorporated Epoxy Coatings on Aluminum Alloy (AA2024). Part 1: Improved Corrosion Performance, *Corros. Sci.*, 2015, **92**, p 118–126
34. W.H. Chang, B. Qu, A.D. Liao, S.F. Zhang, R.F. Zhang, and J.H. Xiang, In Vitro Biocompatibility and Antibacterial Behavior of Anodic Coatings Fabricated in an Organic Phosphate Containing Solution on Mg-1.0Ca Alloys, *Surf. Coat. Technol.*, 2016, **289**, p 75–84
35. M. Jamesh, S. Kumar, and T.S.N. Sankara Narayanan, Corrosion Behavior of Commercially Pure Mg and ZM21 Mg Alloy in Ringer's Solution—Long Term Evaluation by EIS, *Corros. Sci.*, 2011, **53**, p 645–654
36. C.J. Hall, T. Ponnusamy, P.J. Murphy, and M. Lindberg, A Solid-State Nuclear Magnetic Resonance Study of Post-plasma Reactions in Organosilicone Microwave Plasma-Enhanced Chemical Vapor Deposition (PECVD) Coatings, *ACS Appl. Mater. Interfaces*, 2014, **6**, p 8353–8362

37. M.E. Mahmoud, A.E.H. Abdou, and G.M. Nabil, Facile Microwave-Assisted Fabrication of Nano-Zirconium Silicate-Functionalized-3-Aminopropyltrimethoxysilane as a Novel Adsorbent for Superior Removal of Divalent Ions, *J. Ind. Eng. Chem.*, 2015, **32**, p 365–372
38. X.K. Zhong, Q. Li, J.Y. Hu, S.Y. Zhang, B. Chen, S.Q. Xu, and F. Luo, A Novel Approach to Heal the Sol–Gel Coating System on Magnesium Alloy for Corrosion Protection, *Electrochim. Acta*, 2010, **55**, p 2424–2429
39. J. Song and W.J. Van Ooij, Bonding and Corrosion Protection Mechanisms of Gamma APS and BTSE Silane Films on Aluminum Substrates, *J. Adhes. Sci. Technol.*, 2003, **17**, p 2191–2221
40. X.F. Cui, G. Jin, Q.F. Li, Y.Y. Yang, Y. Li, and F.H. Wang, Electroless Ni-P Plating with a Phytic Acid Pretreatment on AZ91D Magnesium Alloy, *Mater. Chem. Phys.*, 2010, **121**, p 308–313
41. Y. Dou, S. Cai, X.Y. Ye, G.H. Xu, K. Huang, X.X. Wang, and M.G. Ren, 45S5 Bioactive Glass–Ceramic Coated AZ31 Magnesium Alloy with Improved Corrosion Resistance, *Surf. Coat. Technol.*, 2013, **228**, p 154–161
42. C.K.S. Pillai and C.P. Sharma, Review Paper: Absorbable Polymeric Surgical Sutures: Chemistry, Production, Properties, Biodegradability, and Performance, *J. Biomater. Appl.*, 2010, **25**, p 291–366
43. D. Wang and G.P. Bierwagen, Sol–Gel Coatings on Metals for Corrosion Protection, *Prog. Org. Coat.*, 2009, **64**, p 327–338
44. A.J. Lopez, J. Rams, and A. Urena, Sol–Gel Coatings of Low Sintering Temperature for Corrosion Protection of ZE41 Magnesium Alloy, *Surf. Coat. Technol.*, 2011, **205**, p 4183–4191
45. N. Leventis, Three-Dimensional Core-Shell Superstructures: Mechanically Strong Aerogels, *Acc. Chem. Res.*, 2007, **40**, p 874–884
46. L.A. Hernandez-Alvarado, L.S. Hernandez, M.A. Lomeli, J.M. Miranda, L. Narvaez, I. Diaz, and M.L. Escudero, Phytic Acid Coating on Mg-Based Materials for Biodegradable Temporary Endoprosthetic Applications, *J. Alloys Compd.*, 2016, **664**, p 609–618
47. T. Kokubo and H. Takadama, How Useful is SBF in Predicting In Vivo Bone Bioactivity?, *Biomaterials*, 2006, **27**, p 2907–2915
48. S.V. Dorozhkin, Calcium Orthophosphate Coatings on Magnesium and Its Biodegradable Alloys, *Acta Biomater.*, 2014, **10**, p 2919–2934
49. S. Shadanbaz and G.J. Dias, Calcium Phosphate Coatings on Magnesium Alloys for Biomedical Applications: A Review, *Acta Biomater.*, 2012, **8**, p 20–30
50. M.G. Ren, S. Cai, G.H. Xu, X.Y. Ye, Y. Dou, K. Huang, and X.X. Wang, Influence of Heat Treatment on Crystallization and Corrosion Behavior of Calcium Phosphate Glass Coated AZ31 Magnesium Alloy by Sol–Gel Method, *J. Non-Cryst. Solids*, 2013, **369**, p 69–75
51. R. Narayanan, S.K. Seshadri, T.Y. Kwon, and K.H. Kim, Calcium Phosphate-Based Coatings on Titanium and Its Alloys, *J. Biomed. Mater. Res. B*, 2008, **85**, p 279–299